Visual Abstract

Heat dissipation and fatigue crack kinetic features of titanium alloy Grade 2 after laser shock peening

A. Iziumova, A. Vshivkov, A. Prokhorov, E. Gachegova
Institute of Continuous Media Mechanics of the Ural Branch of Russian Academy of Science (ICMM UB RAS), Russia
fedorova@icmm.ru, https://orcid.org/0000-0002-1769-9175
vshivkov.a@icmm.ru, http://orcid.org/0000-0002-7667-455X
prokhorov.a@icmm.ru, http://orcid.org/0000-0002-6511-2105
gachegova.e@icmm.ru, https://orcid.org/0000-0001-6849-9889

D. Davydov
Institute of Metal Physics of the Ural Branch of Russian Academy of Sciences (IMP UB RAS), Russia
Ural Federal University (UrFU), Russia
davidov@imp.uran.ru, https://orcid.org/0000-0003-1381-0929

ABSTRACT. The work is devoted to experimental investigation of the laser shock peening (LSP) effect on fatigue crack propagation and heat dissipation at the crack tip in specimens made of titanium alloy Grade 2 with a stress concentrator. It is shown that the LSP can lead both to positive and negative effect on fatigue lifetime. The effective processing scheme, which includes stress concentrator zone, was proposed. This type of treatment forms an optimal residual stress field, which slows down the crack initiation and propagation processes. The effective LSP processing scheme reduces the value of effective stress intensity factor and, as a consequence, effects on intensity of plastic deformation at the crack tip. This effect can be visualized by measurement of heat flux from the crack tip area. Both heat flux from the crack tip and duration of crack initiation are less in the LSP processed specimens. Microstructural investigations of LSP treated material near fatigue crack path have shown that structural defects (twins) that appear on the surface of the material as a result of LSP do not have a significant effect on the fatigue crack propagation, and the configuration of the residual stresses field created by LSP plays a decisive role.

KEYWORDS. Fatigue; Laser shock peening; Heat dissipation; Crack propagation rate; Twins; Residual stress.

OPEN ACCESS

Citation: Iziumova, A., Vshivkov, A., Prokhorov, A., Gachegova, E., Davydov, D., Heat dissipation and fatigue crack kinetic features of titanium alloy Grade 2 after laser shock peening, Frattura ed Integrità Strutturale, 62 (2022) 516-526.

Received: 08.08.2022
Accepted: 09.09.2022
Online first: 12.09.2022
Published: 01.10.2022

INTRODUCTION

The main reasons of metal materials failure and structural degradation are fatigue, corrosion and wear. In most cases, the damage is initiated from the surface of the material. It leads to a decrease in strength properties and rapid propagation of cracks. In this regard, the development of surface hardening methods, search for optimal residual stress configurations and the study of crack propagation features and stages in a hardened material are topical tasks.

One of the most effective and widely used technologies of surface hardening today is laser shock peening (LSP). In contrast to laser heat treating, the processed material is not heated significant during LSP. Hardening occurs by the impact of a shock wave. The effect is achieved due to the characteristic features of laser impact, such as high pressure created in the material (about of tens of GPa), high relative energy density (about of GW/cm^2), ultra-short pulse time (about 10 ns) and high strain rate (reaches 10^7 1/s) [1].

Shock wave generation using high-intensity laser pulses was realized in 1960 [2]. But only relatively recently, with the development of technology, it has become possible to create safe, compact and easy-to-manage high-energy laser systems. LSP technology has become available and competitive. It is effectively used for surface treatment of materials in order to increase their fatigue and strength life, corrosion resistance, as well as to restore working parts subjected to corrosion and fatigue [3–9]. Recently, much attention has been paid to the study of the fatigue properties of a material after LSP, since this technique allows not only to strengthen the surface layer, but also to achieve controllability and high predictability of crack development due to the creation of a certain residual stress field.

The low-cycle fatigue of an AZ80-T6 magnesium alloy blade specimen treated with warm LSP is studied in [10]. Blade specimens were treated by 1064 nm laser with impact frequency of 1–10 Hz, characteristic pulse time of 20 ns, impact energy of 6 J, spot diameter of 5 mm, and relative energy density of 1.54 GW/cm^2. An increase in fatigue life by 11% with LSP and by 76% with warm LSP (30°C) was found compared to the initial state. Works [11, 12] are devoted to the study of structural features after LSP with the aim of the control of physical-mechanical and fatigue properties.

In [13], a numerical model is developed to assess the effect of LSP on crack propagation. This model includes the finite element method and residual stress intensity analysis. An experimental-numerical study of fatigue crack behavior in the Ti-17 titanium alloy is carried out in [14] to define the crack retardation conditions. The optimal mode of LSP including the selection of residual stress fields by changing the intensity of the laser impact energy and coating is proposed in [15] to slow down or stop the fatigue crack growth in specimens of 2024 aluminum alloy. Authors took into account the size and position of the hardened area to balance the induced compressive residual stresses and the resulting tensile residual stresses in order to obtain improved fatigue life and resistance to damage. In [16] authors provide a comprehensive overview of LSP with a focus on the most recent developments in LSP research including warm LSP, electro-pulsing-assisted LSP, cryogenic LSP, LSP without coating, femtosecond LSP and laser peen forming. Additionally, the effect of LSP on the mechanical and microstructural properties of the metallic material and the application of LSP in additive manufactured metals, ceramics, and metallic glasses have been discussed.

LSP allows one to slow down the process of fatigue crack initiation and propagation in the treated material due to the generated compressive residual stress field. It "constrains" the material in stress concentrator area, reduces the effective stress intensity factor (SIF) and reduces plastic deformation in the process zone. It is well known that plastic deformation is accompanied by heat dissipation as a result of the thermoplastic effect [17]. Variation of plastic deformation intensity in the process zone leads to a change of dissipation energy and the energy balance of specimen in general. Thus, the evaluation of energy balance during fatigue crack propagation in a material after LSP allows one to estimate not only the fatigue crack rate (as it is shown in [18]), but the efficiency of compressive residual stress effect on crack propagation. The energy approach is widely used to propose fracture criteria and describe the evolution of fatigue crack [19–25]. Experimental verification of this approach and estimation of the fatigue crack growth rate is based on a reliable measurement of the dissipated energy near the crack tip. To assess the heat dissipation features of fatigue crack propagation through the field of residual compressive stresses, an original contact heat flux sensor has been used [26].

An analysis of literature sources has shown that LSP is a promising technique as for preparing parts with a complex configuration of residual stresses and influence on the crack initiation process, as increasing the fatigue life of metal structural elements. The kinetics of fatigue cracks propagated through the compressive residual stresses field could be described on the base of the energy approach. Energy dissipation reflects the influence of residual stress field on the crack development and it can be used to evaluate the LSP efficiency. Thus, the purpose of this work is to determine the kinetic and thermal characteristics of the fatigue crack propagation in the specimen of titanium alloy Grade 2 treated by LSP, and as well as to evaluate the correlation of these characteristics with residual stresses and microstructural features caused by LSP.

MATERIALS AND EXPERIMENTAL CONDITIONS

Fatigue crack evolution and associated heat dissipation were investigated on specimens of titanium alloy Grade2 without LSP treatment and after LSP. Specimen geometry is shown in Fig. 1A. The chemical composition of the material is presented in Tab. 1.

Ti	Si	Fe	C	O_2	N_2	H_2	Others
Base	0.1	0.25	0.07	0.2	0.04	0.01	0.3

Table 1: Chemical composition of Grade 2 (weight percent).

Before LSP processing both surfaces of studied specimens were polished in several stages by abrasive paper (at the final stage of polishing the grit size does not exceed 3 μm), as it provides a good contact between specimen surfaces and coating. In our case it was aluminum foil. Coating is usually used to avoid damage of structure in surface layer after high intensity laser irradiation.
For LSP processing, we used an original laser setup assembled in the Institute of Continuous Media Mechanics, Ural branch of the Russian Academy of Sciences. The setup includes Nd:YAG high energy laser Beamtech SGR-Extra-10, industrial robotic manipulator STEP SR50 and residual stress measurement system SINT MTS3000 RESTAN. LSP processing was performed on both surfaces of specimens with 2J and 3J laser energy. The laser spot was square with a side of 1 mm. Two LSP scheme presented in Fig. 1B-C were realized to find optimal conditions for improvement of fatigue properties. The arrow in Fig. 1B-C shows the direction of LSP treatment, and color indicates the beginning and finishing of treatment (from red to violet). One layer of LSP treatment was performed. Adjacent square-spots are next to each other without the overlapping region.

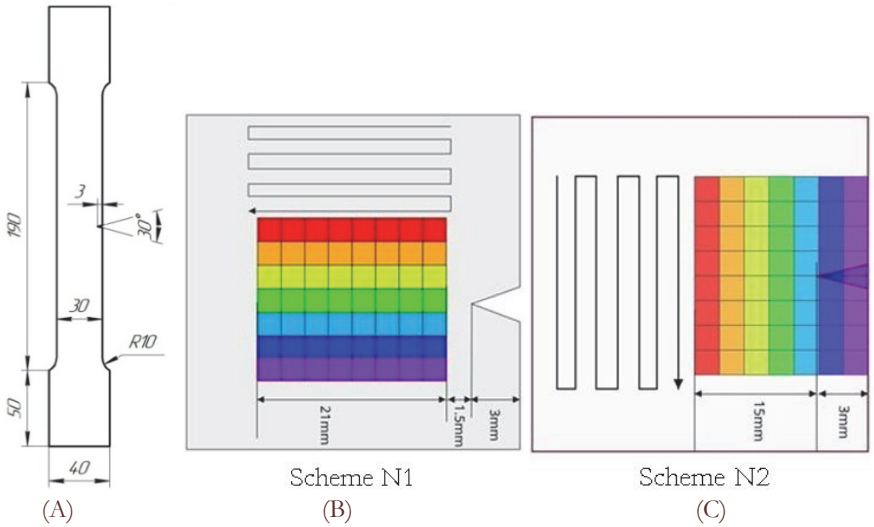

Figure 1: Geometry of studied specimens (all dimensions are in millimeters) (A) and schemes of LSP treatment (B, C).

The main difference between these schemes is that the first scheme (Fig. 1B) didn't include the sharp notch area and during fatigue test the crack was initiated in the untreated material compared to the second scheme (Fig. 1C). The LSP processing in notch area according to the second scheme was performed by special insert in notch to avoid edge effects.
All specimens (including specimens treated by two schemes and base specimens) were tested under uniaxial cyclic loading conditions. Fatigue experiments were carried out on a 100kN servo-hydraulic testing machine Instron 8802 under constant maximum loading of 8 kN at a stress ratio R=0.1 and loading frequency 10 Hz. The direct current potential drop method (PDM) [27] was applied for measuring of crack length. The quantitative measurements of the heat dissipation rate at the crack tip area were carried out using the original heat flux sensor developed by Vshivkov et al. [18]. Tab. 2 presents LSP conditions and result of fatigue test.

Specimen number	Cycles until the end of the test	Scheme of LSP treatment	Laser energy, J
1	102050	Base specimen	0
2	84316	Base specimen	0
9	59471	Scheme N1	3
10	56327	Scheme N1	3
11	215103	Scheme N2	2
12	146722	Scheme N2	3
14	148935	Scheme N2	2

Table 2: Life to failure cycles and LSP characteristics of tested specimens.

Specimens treated by scheme N2 has shown improved results under 2J and 3J of laser energy. Specimens treated by scheme N1 has demonstrated in the least life.

EXPERIMENTAL RESULTS

As a result of experimental work the residual stress profile through the specimen thickness, time dependences of crack length and heat dissipation rate, and specific density of twins versus crack length were obtained.

Residual stress evaluation

LSP technique induces the field of residual stress, which is a combination of compressive and tensile stresses. If this residual stress field has optimal configuration, the duration of crack initiation and propagation will be longer and fatigue properties will be improved. There are a number of ways to measure the residual stress field experimentally such as laboratory X-ray Diffraction, neutron diffraction or synchrotron X-ray Diffraction [28]. In this work, the depth of the residual stress region was examined by incremental hole drilling technique (according to ASTM E837-13a). This technique allows one to visualize and estimate the effectiveness of LSP treatment and to change laser characteristics if necessary. Profiles of residual stresses are presented in Fig. 2A-B. According to these graphs LSP treatment allows one to create residual compression stress field to the depth of approximately 0.9 mm. The maximal compressive stress which plays significant role in control of fatigue crack initiation and propagation, reaches about 750 MPa on depth of approximately 0.3 mm for both schemes of LSP. It is noted that scheme N1 and scheme N2 create approximately the same level and depth of residual stress, and the difference between the two schemes is in location of treated area only.

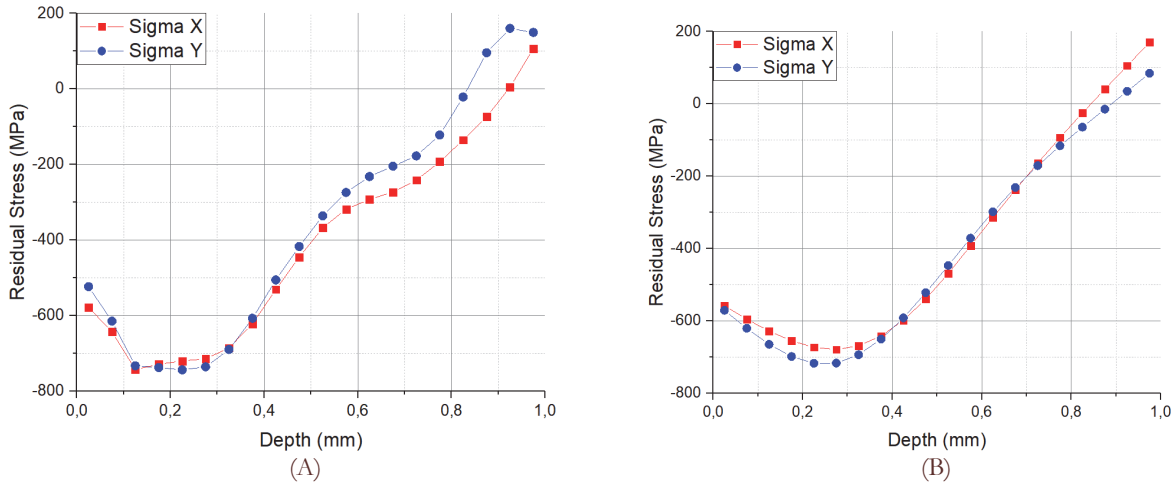

Figure 2: Residual stresses obtained after LSP in specimens of titanium alloy Grade 2 by scheme N1(A) and scheme N2 (B) with laser energy of 3J.

Crack propagation and associated heat dissipation after LSP

Fatigue test was carried out with simultaneous registration of crack length and heat dissipation rate. The original heat flux sensor was used for measurement of heat dissipation rate with accuracy of 1 mW in the range up to 10W. Detailed description of this original technique is presented in [18]. As a result the time dependences of crack length and heat dissipation rate were obtained (Fig. 3A-B). The dependence of crack growth rate and applied SIF range is presented in Fig. 3C.

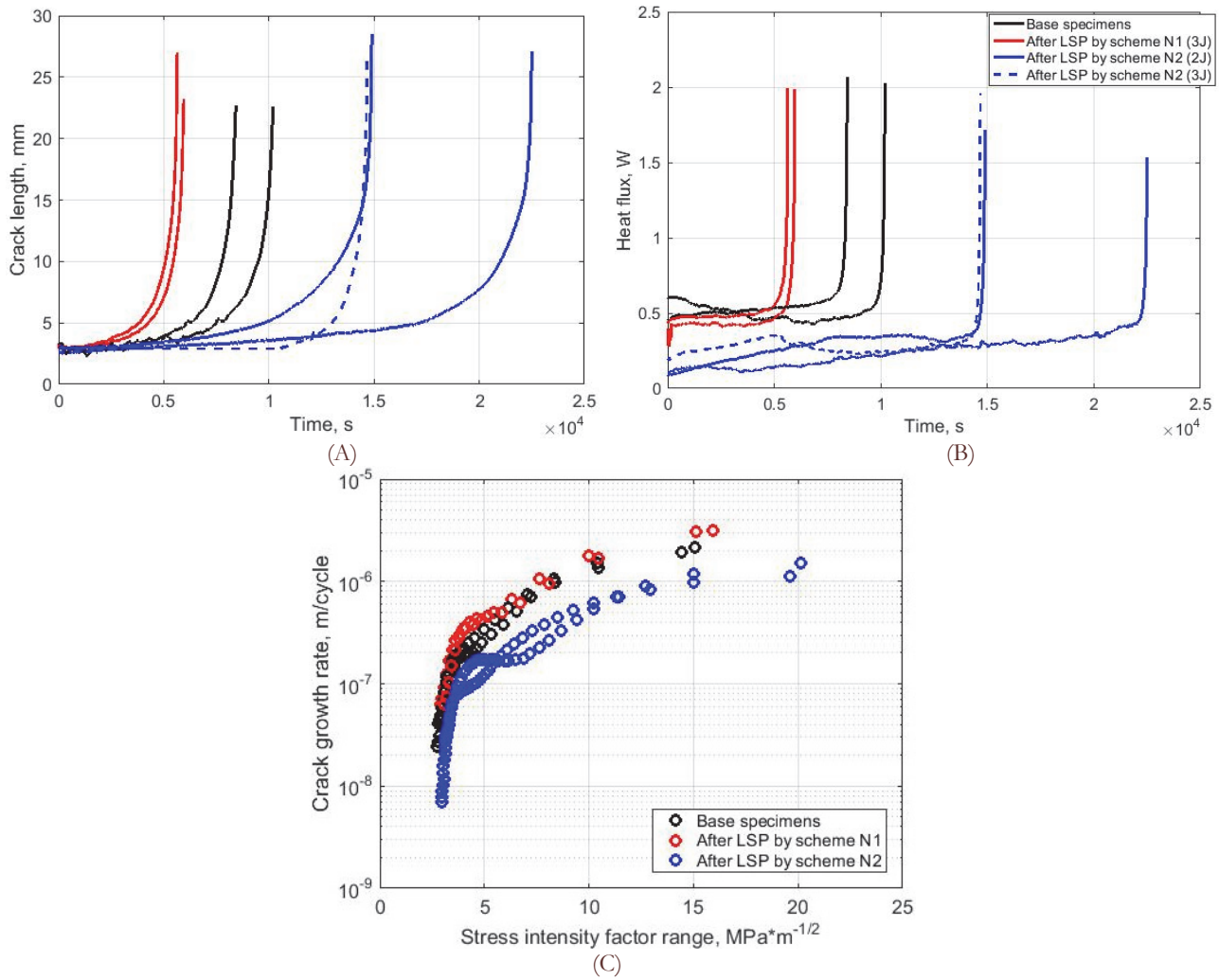

Figure 3: Time dependences of crack length (A), heat dissipation rate (B) and crack growth rate versus applied stress intensity factor range (C).

Three groups of specimens are presented in Fig. 3. Base specimens that have not been LSP processed are indicated by black line. They are the reference against which the change in the fatigue properties of the specimens after LSP processing was evaluated. The second group indicated by red line pertains to specimens after LSP treated according to the scheme N1 (without notch area). In this group crack initiates earlier than in base specimens, the heat dissipation is more intensive. The third group of specimens shown by blue lines in Fig. 3 pertains to specimens after LSP treatment according to the scheme N2 (with notch area). Duration of crack initiation period is significant longer in these specimens than in base specimens, and the heat flux is less intensive. LSP treatment according to the scheme N2 is more appropriate in terms of fatigue properties improvement of titanium alloy Grade2 specimens.

As it was shown in [29-32], the heat dissipation is correlated with stress intensity factor (SIF). In 1970, Elber found that crack closure retards fatigue crack growth rate by reducing the stress intensity range. He introduced the effective stress intensity range for use in Paris' law [33]. Similarly, the effective SIF could be taken in consideration for characterization of crack propagation in residual stress field caused by LSP. In our case, effective SIF is superposition of SIF related to the

applied stress and SIF related to residual stress formed by LSP [34]. Residual stress field is a configuration of tensile and compressive stresses. So that, the created residual stress field can as to increase effective SIF, as to decrease it.
Thus, the effective SIF characterizes residual stresses created by the LSP. At the same time, the effective SIF is related to the intensity of the heat flux. It allows us to estimate the residual stress field formed by the LSP using evolution of the heat flux near the crack tip. According to Fig. 3B, the intensity of heat flux in the crack tip area after the treatment by scheme N1 and without treatment is approximately the same. We can conclude that residual stress field created by scheme N1is not effective for improvement of fatigue properties. In case of scheme N2, the crack is initiated in the compressed material and does not have the ability for intensive development. The heat flux on the specimens processed according to scheme N2 is less that in base material. If the assumption about the relationship between the effective SIF and heat dissipation is correct, then the field of residual stresses created after the LSP according to scheme N2 reduces the effective SIF and, as a result, the heat flux and the crack growth rate decrease.
Fig. 3C presents the dependence of crack growth rate and applied SIF range, calculated by Eqn. (1) [35] for all specimens.

$$\Delta K = \Delta\sigma\sqrt{\pi l}\, f(l,w), \qquad f(l,w) = \frac{5}{20 - 13\alpha - 7\alpha^2}, \qquad \alpha = \frac{l}{w} \tag{1}$$

where $\Delta\sigma$ is applied stress range (Pa), l is crack length (m), $f(l,w)$ is function of crack length l and specimen width w.
With the same applied SIF range, the crack growth rate is lower in specimens after treatment according to scheme N2 comparison with specimens without treatment or after treatment according to scheme N1.
The dependence between heat flux and crack length is presented in Fig. 4. Gray rectangle indicates the area of LSP treatment. Analyzing data of specimens treated by scheme N1 (Fig. 4A), an sudden growth of heat flux begins at a crack length of about 20 mm, while the treatment zone ends at about 25 mm. In Fig. 4B, the plot of heat flux versus crack length has a kink at a crack length of about 15 mm, and the treatment zone ends at 18 mm. Such a discrepancy between the beginning of the heat flux growth and the end of the LSP processing zone can be associated with the edge effect. At the boundary of the treatment zone, a field of tensile residual stresses arises. It accelerates the development of crack and increasing of effective SIF and consequently heat flux.

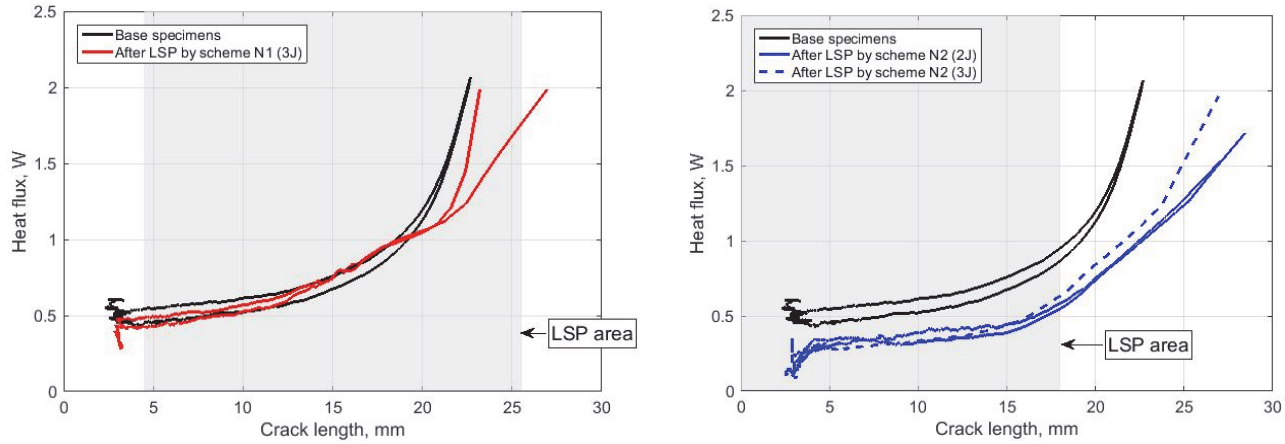

Figure 4: Heat dissipation versus crack length for the specimens processed by scheme N1 (A) and scheme N2 (B). LSP area is colored by gray.

Microstructural analysis of crack propagation zone in stress residual field

Microstructural studies of the crack propagation region of specimen without LSP treatment and with a treated surface were carried out by optical microscopy. Microstructural features were analyzed along the crack in five regions (at the crack tip, ¼ of the crack length, ½ of the crack length, ¾ of the crack length, and at the crack initiation site). Figs. 5-7 show the material microstructure in the area of the crack tip and in the main volume of the material away from crack area obtained on base specimen without LSP processing (Fig. 5) and after LSP processing according to scheme N1 (Fig. 6) and scheme N2 (Fig. 7).

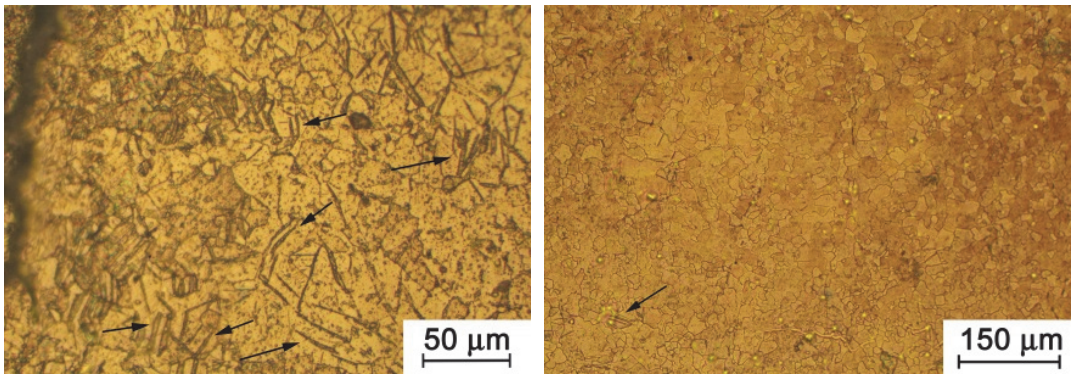

(A) (B)

Figure 5: The microstructure of untreated specimens in crack tip area with magnification of 170x (A) and away from crack tip with magnification of 60x (B). Arrows show twinned grains.

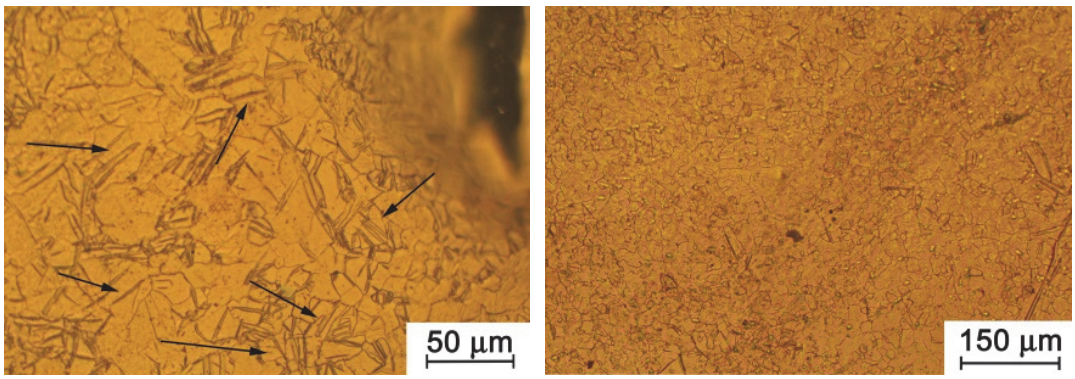

(A) (B)

Figure 6: The structure of specimens after LSP (scheme N1) in crack tip area with magnification of 170x (A) and away from crack tip with magnification of 60x (B). Arrows show twinned grains.

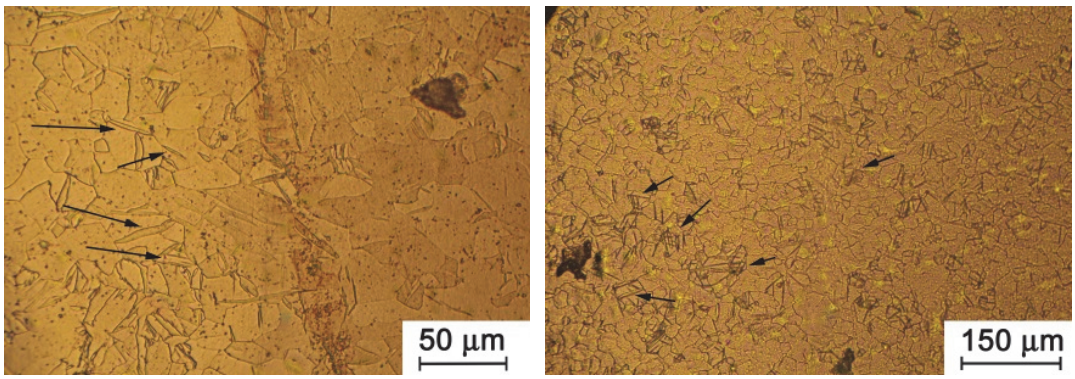

(A) (B)

Figure 7: The structure of specimens after LSP (scheme N2) in crack tip area with magnification of 170x (A) and away from crack tip with magnification of 60x (B). Arrows show twinned grains.

The density of twins along the crack path of reference specimen increases with increasing crack length and reaches its maximum value at the tip; a small amount of twins were found in the main structure of the material. In specimens treated according to scheme N1, the density of twins also increases from the notch to the top. In this case, there are more twinned grains than in the reference specimen both along the crack path and in the base material. A distinctive feature of the structure in specimens processed according to scheme N2 is a significantly larger number of twins than in the reference specimen and specimen processed according to scheme N1. Multiple twinning characterized by a large number of small twins extending from larger ones is observed in scheme N2.

The quantitative analysis of material microstructure included the calculation of twinned grains density in each studied areas. Fig. 8 shows characteristic graphs of the dependence between the twin density and crack length.
The twin density was estimated as the ratio of the twin numbers to the area of the image. It is shown that the twin density on specimen after LSP is higher than on specimen without treatment. LSP treatment is characterized by very large imposed energy, ultra-high strain rate, and ultra-short duration. These conditions have a large effect on microstructure evolution, in particular activation of twinning [36]. Decreasing in twin density on specimens after treatment by scheme N2 could be caused by end of treatment zone which is marked by gray rectangle in Fig.8A. The high value of twin density under crack length about 27 mm (near the edge of specimen) could be connected with developed plastic deformation in crack tip area.

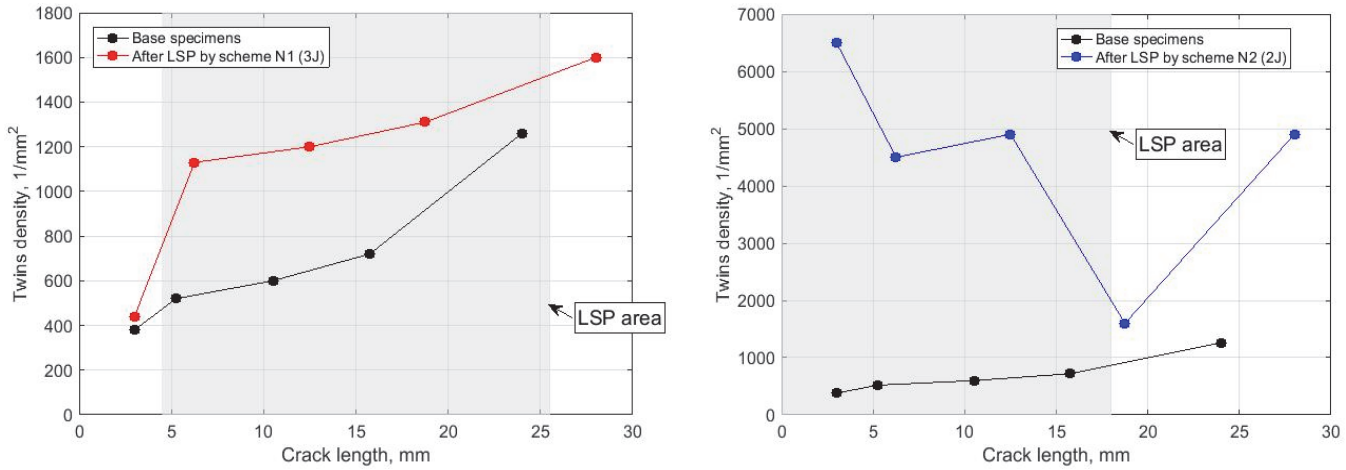

Figure 8: The twin density versus crack length in base specimens and specimens after LSP according to the scheme N1 (A) and scheme N2 (B).

In general, twins can affect the crack growth rate in different ways. In [37] authors investigated the effect of twins in extruded AZ31B magnesium alloy on fatigue crack growth and crack closure behavior. They have found increasing the material deformation and fatigue crack opening displacement due to twins under applied stress ration R=-1. As a result, the effective stress intensity factor range increased, leading to the intensification of fatigue crack growth. From the other hand, at the applied stress ratio R = 0.1, tensile twins were not generated. There was no change in effective stress intensity factor range and no acceleration of FCG. A review on the fatigue cracking of twin boundaries is presented in [38]. Authors approve that the twin boundaries produced by deformation twins in face-centered cubic metals are strong to resist fatigue cracking by promoting deformation homogeneity. In contrast, twin boundaries those linked with deformation twins in hexagonal-close-packed or body-centered-cubic metals are preferential sites for fatigue cracking with strain localization and stress concentration. In our case, the microstructural changes (twins formation) caused by LSP does not significantly effect on the fatigue crack propagation, and the configuration of the residual stress field created by LSP plays a decisive role.

CONCLUSIONS

The LSP technology allows one to increase the fatigue life of metallic materials in the case of optimal choice of LSP processing characteristics such as size and shape of the spot, pulse energy and, most importantly, the LSP treatment scheme. The significant improvement of fatigue life by LSP treatment of specimens with stress concentrator is shown in the case of LSP treatment scheme including region of notch. If the treated zone is spaced relative to the notch tip, the LSP will not effective and the created residual stress field will contribute to the rapid fatigue crack development leading to decrease in the durability of specimens.
An analysis of fatigue crack kinetics and the evolution of heat flux in crack tip area showed that if the LSP zone includes a stress concentrator zone, then the fatigue crack develops more slowly and the heat flux is less intense than in specimen without treatment. This is due to a decrease in effective SIF caused by influence of the residual compressive stress field.

Thus, the heat flux makes it possible to indirectly estimate the change in the effective SIF and the optimality of the created residual stress field.
Microstructural studies have shown that the surface of the material after LSP is more defective compared to the structure of the material without treatment. A significant increase in the density of twinned grains in the LSP treated material was found. At the same time the duration of crack initiation and propagation increases significantly after LSP according to scheme which includes stress concentrator zone. Thus, the structure does not significantly effect on the fatigue crack propagation, and the configuration of the residual stress field created by LSP plays a decisive role. It has to be noted that this configuration includes not only optimal space distribution of residual compressive stress field but corresponding ration of the specimen thickness to the depth of LSP treated layer. This ratio strongly depends on characteristics of laser processing specifically laser energy and laser spot area.

Acknowledgments

This paper was prepared in the framework of the program for the creation and development of the world-class scientific center "Supersonic" for 2020–2025, with the financial support of the Ministry of Education and Science of the Russian Federation.

References

[1] Lu, J., Liu, Y., Luo, K. and Wang, Z. (2018). A kind of uniform strengthening methods of turbine blade subjected to varied square-spot laser shock peening with stagger multiple-layer, United States patent, US2018258509 A1, 13.
[2] Askar'yan, G.A. and Moroz, É.M. (1963). Pressure on Evaporation of Matter in a Radiation Beam, Sov. J. Exp. Theor. Phys., 43, pp. 2319–2320.
[3] Sundar, R., Ganesh, P., Gupta, R.K., Ragvendra, G., Pant, B.K., Kain, V., Ranganathan, K., Kaul, R., Bindra, K.S. (2019). Laser Shock Peening and its Applications: A Review, Lasers Manuf. Mater. Process., 6, pp. 424-463. DOI: 10.1007/s40516-019-00098-8.
[4] Ganesh, P., Sundar, R., Kumar, H., Kaul, R., Ranganathan, K., Hedaoo, P., Tiwari, P., Kukreja, L.M., Oak, S.M., Dasari, S., Raghavendra, G. (2012). Studies on laser peening of spring steel for automotive applications, Opt. Lasers Eng., 50(5), pp. 678–686. DOI: 10.1016/j.optlaseng.2011.11.013.
[5] Ganesh, P., Sundar, R., Kumar, H., Kaul, R., Ranganathan, K., Hedaoo, P., Raghavendra, G., Anand Kumar, S., Tiwari, P., Nagpure, D.C., Bindra, K.S., Kukreja, L.M., Oak, S.M. (2014). Studies on fatigue life enhancement of pre-fatigued spring steel specimens using laser shock peening, Mater. Des., 54, pp. 734–741. DOI: 10.1016/j.matdes.2013.08.104.
[6] Pant, B.K., Sundar, R., Kumar, H., Kaul, R., Pavan, A.H.V., Ranganathan, K., Bindra, K.S., Oak, S.M., Kukreja, L.M., Prakash, R. V., Kamaraj, M. (2013). Studies towards development of laser peening technology for martensitic stainless steel and titanium alloys for steam turbine applications, Mater. Sci. Eng. A, 587, pp. 352–358. DOI: 10.1016/j.msea.2013.08.074.
[7] Gupta, R.K., Sundar, R., Kumar, B.S., Ganesh, P., Kaul, R., Ranganathan, K., Bindra, K.S., Kain, V., Oak, S.M., Kukreja, L.M. (2015). A Hybrid Laser Surface Treatment for Refurbishment of Stress Corrosion Cracking Damaged 304L Stainless Steel, J. Mater. Eng. Perform., 24(6), pp. 2569–2576. DOI: 10.1007/s11665-015-1530-1.
[8] Sundar, R., Ganesh, P., Kumar, B.S., Gupta, R.K., Nagpure, D.C., Kaul, R., Ranganathan, K., Bindra, K.S., Kain, V., Oak, S.M., Singh, B. (2016). Mitigation of Stress Corrosion Cracking Susceptibility of Machined 304L Stainless Steel Through Laser Peening, J. Mater. Eng. Perform., 25(9), pp. 3710–3724. DOI: 10.1007/s11665-016-2220-3.
[9] Gupta, R.K., Sunil Kumar, B., Sundar, R., Ram Sankar, P., Ganesh, P., Kaul, R., Kain, V., Ranganathan, K., Bindra, K.S., Singh, B. (2017). Enhancement of intergranular corrosion resistance of type 304 stainless steel through laser shock peening, Corros. Eng. Sci. Technol., 52(3), pp. 220–5. DOI: 10.1080/1478422X.2016.1254422.
[10] Shanyavskiy, A.A. (2006). Fatigue limit - Material property as an opened or closed system? Practical view on the aircraft components failures in GCF area, Int. J. Fatigue, 28(11), pp. 1647–1657. DOI: 10.1016/j.ijfatigue.2005.12.008.
[11] Umapathi, A., Swaroop, S. (2019). Mechanical properties of a laser peened Ti-6Al-4V, Opt. Laser Technol., 119, pp. 105568. DOI: 10.1016/j.optlastec.2019.105568.
[12] Chen, H., Guan, Y., Zhu, L., Li, Y., Zhai, J., Lin, J. (2021). Effects of ultrasonic shot peening process parameters on nanocrystalline and mechanical properties of pure copper surface, Mater. Chem. Phys., 259, pp. 124025.

DOI: 10.1016/j.matchemphys.2020.124025.
[13] Zhao, J., Dong, Y., Ye, C. (2017). Laser shock peening induced residual stresses and the effect on crack propagation behavior, Int. J. Fatigue, 100, pp. 407–417. DOI: 10.1016/j.ijfatigue.2017.04.002.
[14] Sun, R., Keller, S., Zhu, Y., Guo, W., Kashaev, N., Klusemann, B. (2021). Experimental-numerical study of laser-shock-peening-induced retardation of fatigue crack propagation in Ti-17 titanium alloy, Int. J. Fatigue, 145, pp. 106081. DOI: 10.1016/j.ijfatigue.2020.106081.
[15] van Aswegen, D.C., Polese, C. (2021). Experimental and analytical investigation of the effects of laser shock peening processing strategy on fatigue crack growth in thin 2024 aluminium alloy panels, Int. J. Fatigue, 142, pp. 105969. DOI: 10.1016/j.ijfatigue.2020.105969.
[16] Zhang, C., Dong, Y., Ye, C. (2021). Recent Developments and Novel Applications of Laser Shock Peening: A Review, Adv. Eng. Mater., pp. 2001216. DOI: 10.1002/adem.202001216.
[17] Hodowany, J., Ravichandran, G., Rosakis, A.J., Rosakis, P. (2000). Partition of plastic work into heat and stored energy in metals, Exp. Mech., 40(2), pp. 113–123. DOI: 10.1007/BF02325036.
[18] Vshivkov, A., Iziumova, A., Plekhov, O., Bär, J. (2016). Experimental study of heat dissipation at the crack tip during fatigue crack propagation, Frat. Ed Integrita Strutt., 10(35), pp. 57–63. DOI: 10.3221/IGF-ESIS.35.07.
[19] Chapetti, M.D., Tagawa, T., Miyata, T. (2003). Ultra-long cycle fatigue of high-strength carbon steels part I: Review and analysis of the mechanism of failure, Mater. Sci. Eng. A, 356(1–2), pp. 227–235. DOI: 10.1016/S0921-5093(03)00135-7.
[20] Paris, P., Erdogan, F. (1963). A critical analysis of crack propagation laws, J. Fluids Eng. Trans. ASME, 85(4), pp. 528–533. DOI: 10.1115/1.3656900.
[21] Iino, Y. (1979). Fatigue crack propagation work coefficient-a material constant giving degree of resistance to fatigue crack growth, Eng. Fract. Mech., 12(2), pp. 279–299. DOI: 10.1016/0013-7944(79)90120-6.
[22] Chow, C.L., Lu, T.J. (1991). Cyclic J-integral in relation to fatigue crack initiation and propagation, Eng. Fract. Mech., 39(1), pp. 1–20. DOI: 10.1016/0013-7944(91)90018-V.
[23] Weertman, J. (1973). Theory of fatigue crack growth based on a BCS crack theory with work hardening, Int. J. Fract., 9(2), pp. 125–131. DOI: 10.1007/BF00041854.
[24] Chudnovsky, A. (1985). Thermodynamics of translational crack layer propagation, J. Mater. Sci., 20, pp. 630–635.
[25] Fedorov, V.V. (1979). Thermodynamic aspects of strength and fracture of solids, Tashkent.
[26] Prokhorov, A., Vshivkov, A., Iziumova, A., Plekhov, O., Batsale, J. (2014). Development of the measurement system for determination of dissipation rate near the fatigue crack tip. 12th International Conference on Quantitative Infrared Thermography, Bordeaux, France.
[27] Hartman, G.A., Johnson, D.A. (1987). D-c electric-potential method applied to thermal/mechanical fatigue crack growth, Exp. Mech., 27(1), pp. 106–112. DOI: 10.1007/BF02318872.
[28] S.N van Staden, C. Polese, D. Glaser, J.-P. Nobre, A.M. Venter, D. Marais, J.O. and J.-S.P. (2018).Measurement of Residual Stresses in Different Thicknesses of Laser Shock Peened Aluminium Alloy Samples. Mechanical Stress Evaluation by Neutron and Synchrotron Radiation, 4, pp. 117–22.
[29] Stüwe, H.P., Pippan, R. (1992). On the energy balance of fatigue crack growth, Comput. Struct., 44(1–2), pp. 13–17. DOI: 10.1016/0045-7949(92)90218-O.
[30] Palumbo, D., De Finis, R., Ancona, F., Galietti, U. (2017). Damage monitoring in fracture mechanics by evaluation of the heat dissipated in the cyclic plastic zone ahead of the crack tip with thermal measurements, Eng. Fract. Mech., 181, pp. 65–76. DOI: 10.1016/j.engfracmech.2017.06.017.
[31] Ranc, N., Palin-Luc, T., Paris, P.C. (2011). Thermal effect of plastic dissipation at the crack tip on the stress intensity factor under cyclic loading, Eng. Fract. Mech., 78(6), pp. 961–972. DOI: 10.1016/j.engfracmech.2010.11.010.
[32] Boussattine, Z., Ranc, N., Palin-Luc, T. (2020). About the heat sources generated during fatigue crack growth: What consequences on the stress intensity factor?, Theor. Appl. Fract. Mech., 109, pp. 102704. DOI: 10.1016/j.tafmec.2020.102704.
[33] Elber, W. (1971).The significance of fatigue crack closure. Damage tolerance in aircraft structures. ASTM STP 486, American Society for Testing and Materials, pp. 230–242.
[34] Ruschau, J.J., John, R., Thompson, S.R., Nicholas, T. (1999). Fatigue crack nucleation and growth rate behavior of laser shock peened titanium, Int. J. Fatigue, 21(SUPPL. 1), pp. 199–209. DOI: 10.1016/s0142-1123(99)00072-9.
[35] Murakami, Y. (1990). Stress intensity factors handbook, The Society of Materials Science, Japan, volume 1, p. 51.
[36] Mironov, S., Ozerov, M, Kalinenko, A., Stepanov, N., Plekhov, O., Sikhamov, R., Ventzke, V., Kashaev, N., Salishchev, G., Semiatin, L., Zherebtsov, S. (2022). On the relationship between microstructure and residual stress in laser-shock-peened Ti-6Al-4V, Journal of Alloys and Compounds, 900, pp. 163383.

DOI: 10.1016/j.jallcom.2021.163383.

[37] Masuda, K., Ishihara, S., Oguma, N., Ishiguro, M., Sakamoto, Y. (2021). Effect of twins and plastic-deformation anisotropy of extruded magnesium alloy on fatigue crack growth and crack closure behavior, Materials Science and Engineering: A, 828, pp.142111. DOI: 10.1016/j.msea.2021.142111.

[38]Li, L., Zhang, Z., Zhang, P., Zhang, Z. (2022). A review on the fatigue cracking of twin boundaries: Crystallographic orientation and stacking fault energy, Progress in Materials Science, p.101011. DOI: 10.1016/j.pmatsci.2022.101011.